ISBN: 978-3-95450-214-1 ISSN: 2673-5490 doi:10.18429/JACoW-IPAC2021-MOPAB018

SASE GAIN-CURVE MEASUREMENTS WITH MCP-BASED DETECTORS AT THE EUROPEAN XFEL

E. Syresin†, O. Brovko, A. Grebentsov, Joint Institute for Nuclear Research, Dubna, Russia
M. Yurkov, DESY, Hamburg, Germany
W. Freund, J. Grünert, J. Liu, T. Maltezopoulos, D. Mamchyk
European XFEL GmbH, Hamburg, Germany

Abstract

Radiation detectors based on microchannel plates (MCP) are used for characterization of the Free-Electron Laser (FEL) radiation and measurements of the Self-amplified spontaneous emission (SASE) gain curve at the European XFEL. Photon pulse energies are measured by the MCPs with an anode and by a photodiode. There is one MCP-based detector unit installed in each of the three photon beamlines downstream of the SASE1, SASE2, and SASE3 undulators. MCP detectors operate in a wide dynamic range of pulse energies, from the level of spontaneous emission up to FEL saturation. Their wavelength operation range overlaps with the whole range of radiation wavelengths of SASE1 and SASE2 (from 0.05 nm to 0.4 nm), and SASE3 (from 0.4 nm to 5 nm). In this paper we present results of SASE gain-curve measurements by the MCP-based detectors.

MCP DETECTORS

An important requirement to photon diagnostics [1] at the European XFEL is to provide quick and reliable shot-resolved pulse energy measurements, which can be used for fine online tuning of the FEL amplification process. This requires a detector with a wide dynamic range, controllable tuning to the required wavelength range, and suppression of the spontaneous radiation background (which is rather strong at the European XFEL). The JINR-XFEL collaboration manufactured MCP-based photon detectors as a primary tool for the search of initial signs of SASE and for fine-tuning of the SASE process. Three MCP-based detector units [2, 3] were installed in the European XFEL tunnels, one in each of the photon beamlines downstream of the SASE1, SASE2, and SASE3 undulators.

Three different tasks can be fulfilled with these MCP-based photon detectors [2, 3]: study of the initial stage of the SASE regime, measurement of the photon pulse energy, and measurement of the photon beam image. The MCP detector can resolve each individual pulse at a repetition rate of up to 4.5 MHz, which is the maximum possible intra-pulse train rate of the European XFEL. The MCP-based detectors cover the following wavelength ranges: 0.05-0.4 nm at SASE1 and SASE2 and 0.4-5 nm for SASE3.

The MCP detectors at SASE1 and SASE2 are installed just downstream of the deflecting mirror pair [4-6]. The offset mirrors play an important role for the correct function of the detector. Firstly, they essentially cut higher harmonics of the spontaneous emission radiation, thus reducing the background on the detector. Secondly, they can serve as additional attenuators of the radiation intensity by appropriate tuning of the reflection angle.

The MCP detector for SASE1&SASE2 consists of a silicon photodiode, three MCPs equipped with an anode as pulse energy monitor, and one MCP detector for photon beam imaging. The first MCP detector port houses one silicon photodiode and two F4655 Hamamatsu MCPs of 18 mm outer diameter and 14 mm diameter of active detector area.

The MCP detector for SASE3 has an additional third port upstream of the other two ports. A vacuum manipulator allows inserting to the beam several semi-transparent mesh targets to produce scattered FEL radiation similar to those used at FLASH [7-9].

A CCD camera (Basler avA1600-50gm) with a large field of view of about 90 mm in diameter (MCP diameter of 40 mm and vertical displacement of ±20 mm) and a sufficiently small number of pixels per mm was installed in the BOS-MCP port for recording the phosphor screen image. This camera will allow direct observation of the SASE signature at low intensities. This camera is limited to 10 Hz and thus integrates over the entire pulse trains. A future upgrade is planned to allow fast gating of the BOS-MCP supply high voltages in order to image selectively individual pulses in the pulse trains.

The SASE1 MCP detector was calibrated in the X-ray wavelength range at the DORIS BW1 beamline before installation in the EuXFEL tunnel [10, 11].

The SASE1 MCP was installed in the EuXFEL tunnel in November 2015. The SASE3 MCP was delivered to the EuXFEL tunnel at the end of 2016. The SASE2 MCP detector was installed in the EuXFEL tunnel in 2018 [12].

FIRST SASE MEASHUREMENTS BY MCP DETECTORS

During the first EuXFEL experiments [13] the electron beam had an energy of 14 GeV, the bunch charge was 250 pC, the peak electron current was 5 kA, and the normalized slice emittance was 0.6 mm×mrad. At a photon energy of 9.3 keV, with 500 bunches at 4.5 MHz per bunch train, and an average pulse energy of up to 1.5 mJ, the average power of 6 W of hard X-rays was produced by SASE1 [13].

The SASE3 MCP detectors were commissioned in single- and multi-bunch modes [14-16]. The minimum pulse separation inside an X-ray pulse train of the EuXFEL can be as short as 220 ns. The temporal resolution of the MCP detectors was verified for this case of 4.5 MHz repetition rate by demonstrating clear pulse separation. A fast ADC

12th Int. Particle Acc. Conf. IPAC2021, Campinas, SP, Brazil JACoW Publishing
ISBN: 978-3-95450-214-1 ISSN: 2673-5490 doi:10.18429/JACoW-IPAC2021-MOPAB018

provides the pulse energy in each individual pulse operating at 125 MHz sampling rate.

The absolute values of the SASE radiation pulse energies are obtained by cross-calibration with X-ray Gas Monitors (XGMs) [17, 18]. There are six XGMs in the EuXFEL photon beamlines, which perform online monitoring of the photon beam position and pulse energies. An XGM consists of four vacuum chambers named XGMDh, HAMPh, HAMPv, and XGMDv, which are placed on a common girder. The XGM can record shot-to-shot pulse energies, as well as the absolutely calibrated average (time scale of about 10 seconds) pulse energy and beam position. The XGM is based on photoionization of dilute gases. The photo-ion currents are coupled out directly. The HAMP (Huge Aperture Open Multiplier) is also based on the detection of photo-ions. A repeller accelerates the photo-ions towards a multiplier. This multiplier amplifies the ionic signal to an electron signal, which is electronically amplified and measured with a digitizer.

An example of single-shot SASE3 FEL pulse energies in one train is presented in Fig. 1. The XGM and MCP data panels shown the distribution of the pulse energy over a train of 200 X-ray pulses. Pulse-to-pulse energy fluctuations of the FEL are due to the statistical nature of SASE radiation.

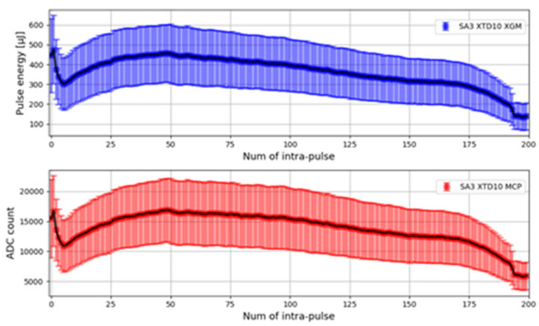

Figure 1: Single-shot SASE3 FEL pulse energies measured by the MCP and XGM for each X-ray pulse of a train of 200 pulses.

The SASE 3 pulse energy measurements by the MCP and XGM detectors for different trains are given in Fig.2. There is good agreement between the MCP and XGM data. The linear correlation of the MCP and XGM pulse energy signals is presented in Fig. 3.

The MCP detectors were used for gain curve measurements at SASE2. The FEL pulse energy versus the number of active undulator cells is shown in Fig.4. The length of each undulator module is 5 m, and each undulator cell has the length of 6.1 m which includes a segment and an intersection.

MCP pulse energy measurements (red line is MCP mean data) were performed by increasing the MCP voltage while decreasing the number of active undulator cells (green line). The MCP voltage is 1800 V for 2 undulator cells (at the level of spontaneous emission). The MCP voltage is 1240 V for undulator cells from 17 to 28, which corresponds to the saturation regime.

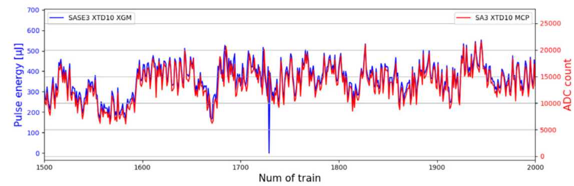

Figure 2: SASE3 FEL pulse energy measured by the MCP and XGM over 6000 consecutive pulse trains.

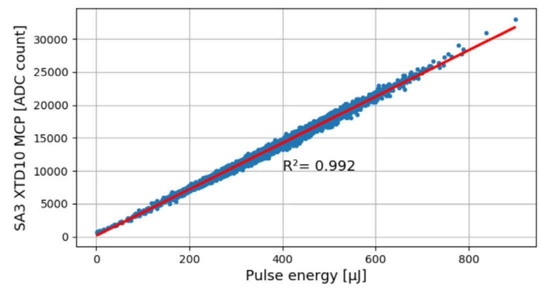

Figure 3: Correlation plot of average MCP and XGM signals.

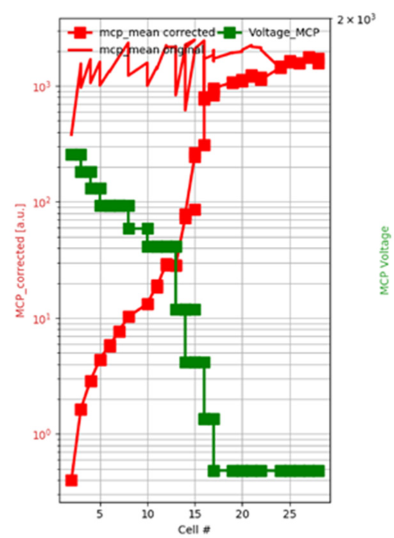

Figure 4: Dependence of the MCP pulse energy signal (red squares) and the MCP voltage (green squares) on the number of active (closed) SASE 2 undulator cells. The uncorrected raw data (red line without symbols) is shown for reference where the MCP gain was changed.

The MCP gain versus the MCP voltage was obtained in these and previous calibration measurements [9]. The measured gain curve was obtained on the basis of the raw MCP data and calibration measurements by measuring twice - before and after each MCP voltage change - at each cell where the MCP voltage had to be changed to increase gain due to largely decreasing signal levels at reducing number of active cells. The saturation regime is obtained with 17 active undulator cells.

A comparison of the measured gain curves performed by the MCP and XGM detectors is presented in Fig. 5. The XGM gain curve measurements are performed with the two different diagnostic subcomponents XGMD and HAMP. The XGMD photon flux (in green) is the abso-

ISBN: 978-3-95450-214-1 ISSN: 2673-5490 doi:10.18429/JACoW-IPAC2021-MOPAB018

lutely calibrated average (in a timescale of about 10 seconds) pulse energy in µJ. In single-bunch mode, the XGMD is not sufficient to perform gain measurements with a small number of active undulator cells since they produce only a low FEL pulse energy compared to the spontaneous emission background at the initial exponential part of the gain curve. However, the XGMD photon flux data is in good agreement with the HAMP signals (in red) when the pulse energy is over 100 µJ.

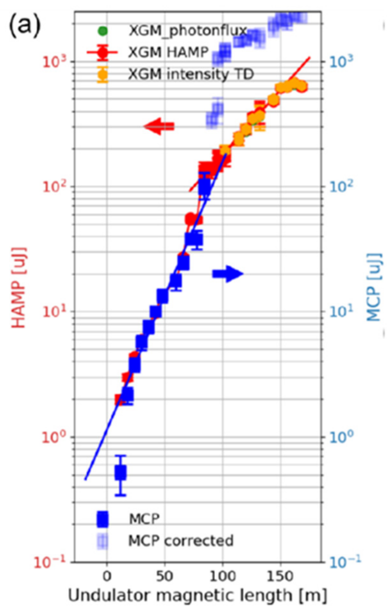

Figure 5: The dependence of corrected MCP pulse energy (blue), corrected HAMP (red) and XGM photon flux (in green) and the mean value of the pulse-resolved XGM data on SASE 2 undulator length.

The HAMP and MCP gain curve data are in good agreement at the exponential part where pulse energy is lower than 100 µJ. When undulator length is about 90 m, the HAMP indicates a transition to the SASE saturation regime. The MCP data show that the SASE saturation regime starts when the undulator length is about 100 m. This first measurement with MCP, HAMP and XGMD of the SASE2 gain curve is planned to be repeated in the near future.

REFERENCES

[1] J. Grünert *et al.*, "X-Ray Photon Diagnostics at the European XFEL", *J. Synchrotron Rad.*, vol. 26, pp. 1422-1431, 2019. doi:10.1107/S1600577519006611

[2] E. Syresin *et al.*, "Development of MCP Based Photon Detectors for the European XFEL", in *Proc. 2nd Int. Particle Accelerator Conf. (IPAC'11)*, San Sebastian, Spain, Sep. 2011, paper TUPC121, pp. 1299-1301.

[3] O. Syresin *et al.*, "Diagnostic technique with femtosecond resolution applied for FEL electron bunches", in *Proc. 23 rd Russian Particle Accelerator Conf. (RUPAC'12)*, Saint Petersburg, Russia, Sep. 2012, paper WEPPD003, pp. 572-574.

[4] J. Grünert, "Photon Diagnostics Requirements and Challenges at the European XFEL", in *Proc. 31st Int. Free Electron Laser Conf. (FEL'09)*, Liverpool, UK, Aug. 2009, paper MOPC56, pp. 146-148.

[5] H. Sinn *et al.*, "Design of Photon Beamlines at the European XFEL", in *Proc. 32nd Int. Free Electron Laser Conf. (FEL'10)*, Malmö, Sweden, Aug. 2010, paper THOCI1, pp. 683-689.

[6] H. Sinn *et al.*, "Technical Design Report: X-ray Optics and Beam Transport", Hamburg, Germany, XFEL.EU TR-2012-006, 2012. doi:10.3204/XFEL-EU/TR-2012-006

[7] B. Fatz *et al.*, "Alignment of the optical feedback system of VUV regenerative FEL amplifier at the TESLA test facility at DESY", *Nucl. Inst. Meth.* A, vol. 483, pp. 412-417, 2002. doi:10.1016/S0168-9002(02)00353-4

[8] A. Bytchkov *et al.*, "Development of MCP based photondiagnostics at the TESLA Test Facility at DESY", *Nucl. Inst. Meth.* A, vol. 528, pp. 254-257, 2004. doi:10.1016/j.nima.2004.04.058

[9] O. I. Brovko *et al.*, "MCP-based Photon Detector with Extended Wavelength Range for FLASH", in *Proc. 29th Int. Free Electron Laser Conf. (FEL'07)*, Novosibirsk, Russia, Aug. 2007, paper WEPPH007, pp. 334-337.

[10] E. Syresin *et al.*, "Synchrotron Radiation Test Validations of European XFEL MCP-based Detectors at DORIS Beamline BW1", in *Proc. 5th Int. Particle Accelerator Conf. (IPAC'14)*, Dresden, Germany, Jun. 2014, paper WEPRO094, pp. 2180-2182. doi:10.18429/JACoW-IPAC2014-WEPRO094

[11] E. Syresin *et al.*, "Radiation detectors based on microchannel plates for free electron lasers", *Physics of Particle and Nuclei Letters,* vol. 11, no. 6, pp. 730-736, 2014. doi:10.1134/S1547477114060144

[12] E. Syresin *et al.*, "MCP Based Detectors Installation in European XFEL", in *Proc. 8th Int. Particle Accelerator Conf. (IPAC'17)*, Copenhagen, Denmark, May 2017, paper THPAB132, pp. 4031-4033. doi:10.18429/JACoW-IPAC2014-WEPRO094

[13] M. Koepke *et al.*, "A MHz-repetition-rate hard X-ray free-electron laser driven by a superconducting linear accelerator", *Nature photonics,* vol. 14, pp. 391-397, 2020. doi:10.1038/s41566-020-0607-z

[14] E. Syresin *et al.*, "MCP Based Detectors of European XFEL", in *Proc. 10th Int. Particle Accelerator Conf. (IPAC'19)*, Melbourne, Australia, May 2019, paper THPGW051, pp. 3703-3705. doi:10.18429/JACoW-IPAC2019-THPGW051

[15] E. Syresin *et al.*, "MCP-based detectors: calibration and first photon radiation measurements", *J. Synchrotron Rad.*, vol. 26, pp. 1400-1405, 2019. doi:10.1107/S1600577519006295

[16] A. Grebentsov *et al.*, "MCP – based Detectors, Calibration, Acceptance Tests, and First Photon Radiation Measurements", in *Proc. 5th Int. Workshop New Photon-Detectors (PD18)*, *JPS Conf. Proc.*, Tokyo, Japan, 2019, vol. 27, pp. 012008-1-012008-5. doi:10.7566/JPSCP.27.012008

[17] A. A. Sorokin *et al.*, "An X-ray gas monitor for free-electron lasers", *J. Synchrotron Rad.*, vol. 26, pp. 1092-1100, 2019. doi:10.1107/S1600577519005174

[18] Th. Maltezopoulos *et al.*, "Operation of X-ray monitors at the European XFEL", *J. Synchrotron Rad.* vol. 26, pp. 1045-1051, 2019. doi:10.1107/S1600577519005174